JACS
JOURNAL OF THE AMERICAN CHEMICAL SOCIETY
Communication
pubs.acs.org/JACS

Transition States of Vicinal Diamine-Catalyzed Aldol Reactions

Adam Simon, Yu-hong Lam, and K. N. Houk*

Department of Chemistry and Biochemistry, University of California, Los Angeles, 607 Charles E. Young Drive East, Los Angeles, California 90095-1569, United States

Supporting Information

ABSTRACT: The transition states of aldol reactions catalyzed by vicinal diamines are characterized with density functional calculations. It was found that a cyclic transition state involving a nine-membered hydrogen-bonded ring is preferred. The crown (chair−chair) conformations of the transition state account for the observed stereoselectivity of these reactions.

Vicinal diamines such as **1**−**5** are effective organocatalysts for aldol reactions.[1−4] The pioneering work by Yamamoto with catalyst **1** was one of the first examples of chiral diamines in direct aldol reactions.[5] Luo followed this with the first effective chiral primary-tertiary diamine catalyst **2**.[6] Zhang computationally investigated the stereoselectivity of aldol reactions with diamine **2**.[7] The origins of stereoselectivities in these reactions were explained by *ad hoc* models with steric clashes between the substrate and the catalyst moieties. The nature of the transition states in these reactions and their role in determining stereocontrol have received little attention.

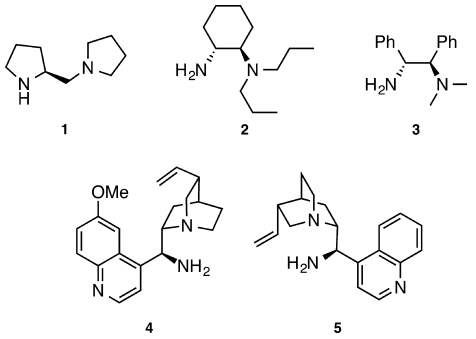

We recently studied the origins of enantiocontrol in the organocatalyzed fluorination[8,9] and an intramolecular aldol condensation,[10,11] both catalyzed by cinchona alkaloid-derived primary amines that contain a chiral vicinal diamine. We showed that these reactions proceed through cyclic transition states with well-defined conformations. We have now investigated the origins of stereoselectivity in intermolecular aldol reactions catalyzed by vicinal diamines. Here, we propose cyclic transition structures for these reactions and show how their conformational preferences underlie the high levels of stereoselectivity in a manner that is reminiscent of the seminal Zimmerman−Traxler model.[12]

The model by Zimmerman and Traxler was a breakthrough in the understanding of stereocontrol in aldol additions. The stereochemical outcomes of metal-catalyzed aldol reactions are governed by the conformation of a six-membered cyclic transition state (Figure 1A).[12,13] The conformational preference

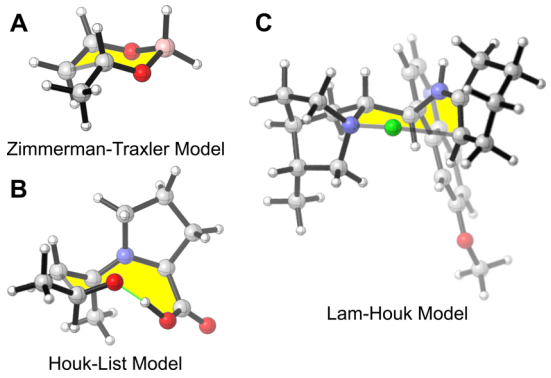

Figure 1. Example of the Zimmerman−Traxler model (A), the Houk−List model with L-proline (B), and the Lam−Houk model with cinchona alkaloid-primary amine (C).

of cyclic transition states has since then been the basis of stereocontrol in a wide variety of asymmetric reactions. In the Houk−List model for proline-catalyzed aldol reactions, the stereochemistry-determining C−C bond-forming step involves a partial Zimmerman−Traxler-like transition state acquiring a chair configuration of the enamine and the electrophilic carbonyl group (Figure 1B).[14] The intramolecular fluorine transfer in Figure 1C acquires a chair conformation of the seven-membered stereocontrolling cyclic transition state.[8] The transition state models summarized in Figure 1 highlight the chair transition states of these asymmetric reactions.

We first explored the simplest possible example of aldol transition states for the aldol reaction acetaldehyde and formaldehyde catalyzed by ethylenediamine, the parent vicinal diamine (Scheme 1). We also studied the experimental system of acetone and *p*-nitrobenzaldehyde catalyzed by diamine **1**.

Conformational searches were performed with OPLS-2005 force-fields in Maestro/Macromodel.[15] Quantum chemical calculations were performed using Gaussian 09.[16] Geometry optimizations and frequency calculations were performed at the B3LYP/6-31G(d) level of theory.[17] Single-point energies of the aldol transition structures were also calculated using B3LYP,[17] ωB97X-D,[18] and M06-2X[19] with the def2-TZVPP[20] basis set in conjunction with the IEF-PCM[21] solvation model for the experimental system. The M06-2X/def2-TZVPP//B3LYP/6-

Received: November 18, 2015
Published: January 4, 2016

ACS Publications © 2016 American Chemical Society

DOI: 10.1021/jacs.5b12097
J. Am. Chem. Soc. 2016, 138, 503−506

Scheme 1. Model Aldol Reaction and Yamamoto's Reported Aldol Addition Catalyzed by L-Proline Derived Catalyst

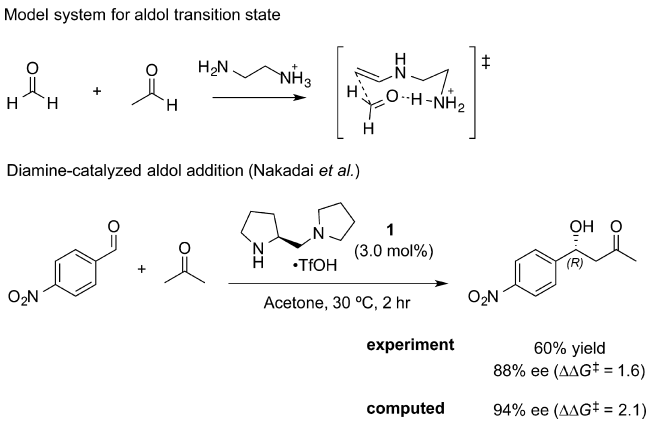

31G(d) level of theory, including IEF-PCM (acetone) for the experimentally used solvent, has been shown to efficiently yield accurate energies for stereoisomeric transition states in organocatalytic systems,[22] and the results using this method are presented in the main text. All other DFT methods (see Table S1) yielded the same trends and magnitudes in the relative free energies of activation ($\Delta\Delta G^{\ddagger}$) of the stereoisomeric transition structures.

The four lowest-energy transition structures for the aldol reaction of formaldehyde and acetaldehyde catalyzed by protonated ethylenediamine are shown in Figure 2. These four are (+)-gauche diamines. There are four enantiomeric structures with (−)-gauche diamine conformers as well.

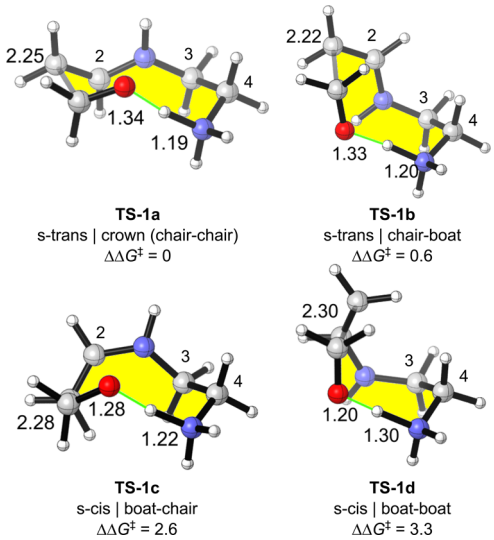

Figure 2. Lowest-energy transition structures **TS-1a–d** for the aldol addition of formaldehyde and the enamine formed by (+)-gauche ethylenediamine and acetaldehyde (M06-2X/def2-TZVPP//B3LYP/6-31G(d)). The free energies of activation ($\Delta\Delta G^{\ddagger}$), relative to **TS-1a**, are reported in kcal/mol.

The cyclic transition structures are highlighted in yellow. As in the intramolecular aldol study,[10] the eight heavy atoms of the aldol transition state resemble low-energy conformers of cyclooctane.[23] **TS-1a** is the crown conformation (chair−chair) and is the lowest-energy transition structure. **TS-1b** is the chair−boat and is higher in energy than **TS-1a** by only 0.6 kcal/mol. **TS-1a** and **TS-1b** both acquire Zimmerman−Traxler chair conformations,[12] but **TS-1b** is a boat on the catalyst side. The dihedral angle of the N−C3−C4−N bond is 58° for **TS-1a** and 55° for **TS-1b**, corresponding to a favorable conformation of the catalyst. The minor difference in energy between the two transition structures arises from an eclipsed H−H interaction in **TS-1b** between the N−H of the enamine and the axial C−H of C3. Both **TS-1a** and **TS-1b** have s-trans configurations of the enamine and staggered approaches along the forming C−C bond.

TS-1c is in a boat−chair conformation and is 2.6 kcal/mol higher in energy than **TS-1a**. **TS-1d** is in a boat−boat conformation and is 3.3 kcal/mol higher in energy compared to **TS-1a**. Both transition structures have s-cis configurations of the enamine and are higher in energy than the s-trans transition structures, in agreement with the Houk−List model.[14] The destabilization of both **TS-1c** and **TS-1d** is due to eclipsing about the forming C−C bond, a type of torsional steering.[24] The presence of 1,2-allylic strain of the enamine NH and vinyl hydrogen of C2 also contributes to their higher energies. Additionally, the dihedral angle of the N−C3−C4−N bond is 75° for **TS-1c** and 46° for **TS-1d**. Both transition structures have boat conformations at the forming C−C bond and are higher in energy compared to the chairs (**TS-1a** and **TS-1b**), as in the Zimmerman−Traxler model.[12] In addition to these four transition structures, four higher-energy conformations were located (see Figure S1).

These results show that there are strongly preferred crown (chair−chair) and chair−boat conformations. For the experimental catalysts **1**–**5**, the (+)- or (−)-gauche preference is determined by the chirality of the catalyst, which excludes the possibility of enantiomeric conformations. We explored if the conformational preferences observed in the model system are maintained in more substituted systems with catalyst **1**.

We studied the Yamamoto catalyst **1** that attained reasonable stereoselectivity in an intermolecular aldol addition of *p*-nitrobenzaldehyde and acetone (Scheme 1). Enantioselectivity in this reaction is 88% ee, which corresponds to a difference in activation free energies ($\Delta\Delta G^{\ddagger}$) of 1.6 kcal/mol. The two lowest-energy transition structures leading to the major (**TS-2a**) and minor (**TS-2b**) products are illustrated in Figure 3. **TS-2a** and **TS-2b** have (+)-gauche conformations of the catalyst and are both crown conformations. They differ in the facial selectivity of

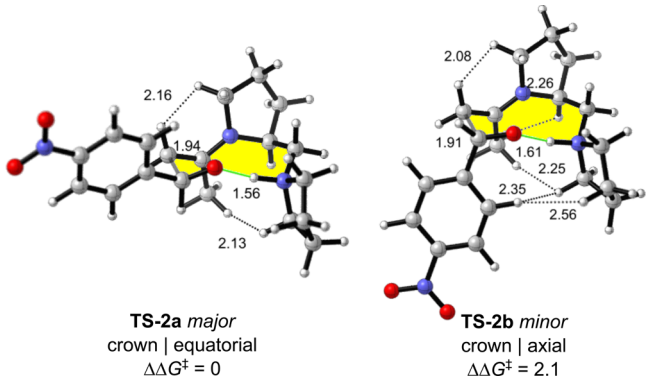

Figure 3. Lowest-energy transition structures **TS-2a** and **TS-2b** for the aldol addition of *p*-nitrobenzaldehyde and the enamine formed by catalyst **1** and acetone (M06-2X/def2-TZVPP−IEF-PCM(acetone)//B3LYP/6-31G(d)−IEF-PCM(acetone)). The free energies of activation ($\Delta\Delta G^{\ddagger}$), relative to **TS-2a**, are reported in kcal/mol.

DOI: 10.1021/jacs.5b12097
J. Am. Chem. Soc. 2016, 138, 503−506

the aldehyde: **TS-2a** has an equatorial aryl group, and **TS-2b** has an axial aryl group. The geometry of the enamine catalyst is very similar in both transition structures. Thus, the enantioselectivity arises from the equatorial versus axial position of the aldehyde substituent on a cyclic transition state in the crown conformation.

In addition to **TS-2a** and **TS-2b**, 7 stereoisomeric transition structures **TS-2c–i** were located (Figure 4). **TS-2c**, **TS-2e**, and

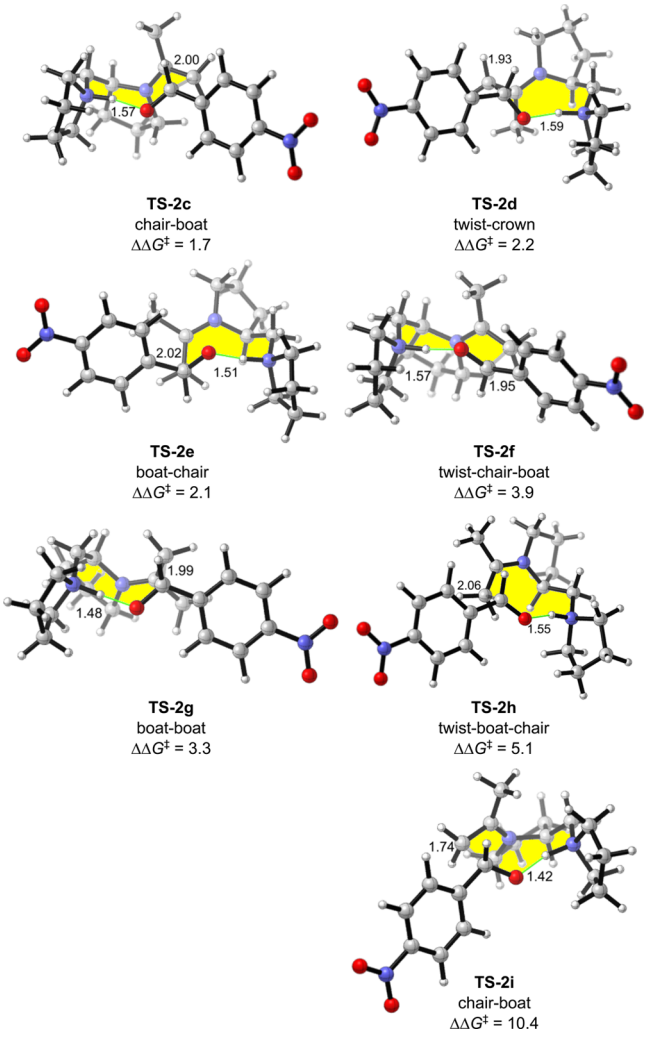

Figure 4. Transition structures **TS-2c–i** for the aldol reaction of *p*-nitrobenzaldehyde and the enamine formed by catalyst **1** and acetone (M06-2X/def2-TZVPP–IEF-PCM(acetone)//B3LYP/6-31G(d)–IEF-PCM(acetone)). Stereoisomeric transition structures that lead to the major (*R*) product are on the left side of the figure. Stereoisomeric transition structures that lead to the minor (*S*) product are on the right side of the figure. The relative free energies of activation compared with **TS-2a** are reported in kcal/mol.

TS-2g lead to the major (*R*) enantiomer, while **TS-2d**, **TS-2f**, **TS-2h**, and **TS-2i** lead to the minor (*S*) enantiomer. **TS-2c**, **TS-2f**, and **TS-2g** have (−)-gauche conformations at the NCCN bond of the diamine, and the pyrrolidine rings are axial relative to the cyclic aldol transition state. **TS-2d**, **TS-2f**, **TS-2g**, and **TS-2h** are destabilized due to eclipsed forming C–C bonds. **TS-2e** is higher in energy than **TS-2a** by 2.1 kcal/mol and is in the boat-chair conformation that is destabilized by a slightly eclipsed forming C–C bond and a wide 79° NCCN dihedral angle of the catalyst. **TS-2i**, a chair–boat but with a highly distorted pyrrolidine ring, is 10.4 kcal/mol higher in energy.

We have found that the lowest-energy transition structures, i.e. the crown (chair–chair) conformations, acquire matching (+)-gauche conformations at both the forming C–C bond and the NCCN bond of the catalyst. The catalyst is able to occupy both (+)- and (−)-gauche conformations at the NCCN bond, however the (+)-gauche conformations were found to be more stable in this case because the (−)-gauche conformer has an axial pyrrolidine ring. The transition structures with mismatching (+)- and (−)-gauche conformations are higher in energy. The model system is quite transferable to the experimental system. The RMSD between the skeleton of the crown in the model and experimental system was 0.13 Å.

The stereoselectivity of intermolecular aldol additions catalyzed by vicinal diamines can be explained by the model in Scheme 2. The hydrogen-bonded transition state prefers a crown

Scheme 2. Stereoselectivity Model for Vicinal Diamine-Catalyzed Aldol Reactions

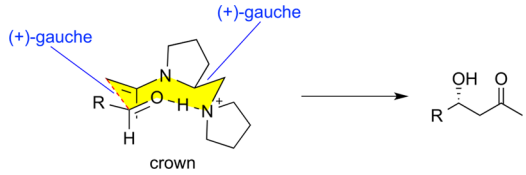

conformation, although the chair–boat is only slightly higher in energy. Both the crown and the chair–boat contain a chair arrangement of the enamine and carbonyl atoms that is consistent with the Zimmerman–Traxler model. These preferences are found in the model system and are amplified in substituted systems with additional steric interactions. In the intramolecular aldol condensation,[10] we found that the stereocontrolling transition structure was the boat–chair. In that case, the presence of a tether between the enamine and carbonyl affected the approaching C–C bond configurations, which led to the boat-chair acquiring a more favorable staggered conformation. The bimolecular aldol additions with more complex diamine catalysts such as **2**, **4**, and **5** are currently under investigation.

■ ASSOCIATED CONTENT

Supporting Information

The Supporting Information is available free of charge on the ACS Publications website at DOI: 10.1021/jacs.5b12097.

Complete set of model aldol transition structures and their energies. Computational results by other density functionals for the model system. Cartesian coordinates and thermodynamic parameters (in hartrees) of all stationary points (PDF)

■ AUTHOR INFORMATION

Corresponding Author

*houk@chem.ucla.edu

Notes

The authors declare no competing financial interest.

■ ACKNOWLEDGMENTS

Financial support is provided by the National Science Foundation (CHE-1361104). A.S. is a recipient of the NIH

DOI: 10.1021/jacs.5b12097
J. Am. Chem. Soc. 2016, 138, 503–506

Chemistry-Biology Interface Research Training Grant (USPHS National Research Service Award T32GM008496). The computational resources from the UCLA Institute of Digital Research and Education are gratefully acknowledged.

REFERENCES

(1) Li, J.; Fu, N.; Li, X.; Luo, S.; Cheng, J.-P. *J. Org. Chem.* **2010**, *75*, 4501.
(2) Chen, L.; Luo, S.; Li, J.; Li, X.; Cheng, J.-P. *Org. Biomol. Chem.* **2010**, *8*, 2627.
(3) Gao, J.; Bai, S.; Gao, Q.; Liu, Y.; Yang, Q. *Chem. Commun.* **2011**, *47*, 6716.
(4) Kumar, A.; Singh, S.; Kumar, V.; Chimni, S. S. *Org. Biomol. Chem.* **2011**, *9*, 2731.
(5) Nakadai, M.; Saito, S.; Yamamoto, H. *Tetrahedron* **2002**, *58*, 8167.
(6) (a) Luo, S.; Xu, H.; Li, J.; Zhang, L. A.; Cheng, J.-P. *J. Am. Chem. Soc.* **2007**, *129*, 3074. (b) Zhang, L.; Fu, N.; Luo, S. *Acc. Chem. Res.* **2015**, *48*, 986.
(7) Sun, X.; Zhu, R.; Gao, J.; Zhang, D.; Feng, D. *J. Phys. Chem. A* **2012**, *116*, 7082.
(8) Lam, Y.-h.; Houk, K. N. *J. Am. Chem. Soc.* **2014**, *136*, 9556.
(9) Kwiatkowski, P.; Beeson, T. D.; Conrad, J. C.; MacMillan, D. W. C. *J. Am. Chem. Soc.* **2011**, *133*, 1738.
(10) Lam, Y.-h.; Houk, K. N. *J. Am. Chem. Soc.* **2015**, *137*, 2116.
(11) Zhou, J.; Wakchaure, V.; Kraft, P.; List, B. *Angew. Chem., Int. Ed.* **2008**, *47*, 7656.
(12) Zimmerman, H. E.; Traxler, M. D. *J. Am. Chem. Soc.* **1957**, *79*, 1920.
(13) Li, Y.; Paddon-Row, M. N.; Houk, K. N. *J. Am. Chem. Soc.* **1988**, *110*, 3684.
(14) Bahmanyar, S.; Houk, K. N.; Martin, H. J.; List, B. *J. Am. Chem. Soc.* **2003**, *125*, 2475.
(15) (a) Banks, J. L.; Beard, H. S.; Cao, Y.; Cho, A. E.; Damm, W.; Farid, R.; Felts, A. K.; Halgren, T. A.; Mainz, D. T.; Maple, J. R.; Murphy, R.; Philipp, D. M.; Repasky, M. P.; Zhang, L. Y.; Berne, B. J.; Friesner, R. A.; Gallicchio, E.; Levy, R. M. *J. Comput. Chem.* **2005**, *26*, 1752. (b) Schrödinger Release 2015-3: *MacroModel*, version 10.9; Schrödinger, LLC: New York, 2015.
(16) Frisch, M. J.; Trucks, G. W.; Schlegel, H. B.; Scuseria, G. E.; Robb, M. A.; Cheeseman, J. R.; Scalmani, G.; Barone, V.; Mennucci, B.; Petersson, G. A.; Nakatsuji, H.; Caricato, M.; Li, X.; Hratchian, H. P.; Izmaylov, A. F.; Bloino, J.; Zheng, G.; Sonnenberg, J. L.; Hada, M.; Ehara, M.; Toyota, K.; Fukuda, R.; Hasegawa, J.; Ishida, M.; Nakajima, T.; Honda, Y.; Kitao, O.; Nakai, H.; Vreven, T.; Montgomery, J. A., Jr.; Peralta, J. E.; Ogliaro, F.; Bearpark, M.; Heyd, J. J.; Brothers, E.; Kudin, K. N.; Staroverov, V. N.; Keith, T.; Kobayashi, R.; Normand, J.; Raghavachari, K.; Rendell, A.; Burant, J. C.; Iyengar, S. S.; Tomasi, J.; Cossi, M.; Rega, N.; Millam, J. M.; Klene, M.; Knox, J. E.; Cross, J. B.; Bakken, V.; Adamo, C.; Jaramillo, J.; Gomperts, R.; Stratmann, R. E.; Yazyev, O.; Austin, A. J.; Cammi, R.; Pomelli, C.; Ochterski, J. W.; Martin, R. L.; Morokuma, K.; Zakrzewski, V. G.; Voth, G. A.; Salvador, P.; Dannenberg, J. J.; Dapprich, S.; Daniels, A. D.; Farkas, O.; Foresman, J. B.; Ortiz, J. V.; Cioslowski, J.; Fox, D. J. *Gaussian 09*, Rev. D.01; Gaussian, Inc.: Wallingford, CT, 2013.
(17) (a) Becke, A. D. *J. Chem. Phys.* **1993**, *98*, 5648. (b) Lee, C.; Yang, W.; Parr, R. G. *Phys. Rev. B: Condens. Matter Mater. Phys.* **1988**, *37*, 785. (c) Vosko, S. H.; Wilk, L.; Nusair, M. *Can. J. Phys.* **1980**, *58*, 1200. (d) Stephens, P. J.; Devlin, F. J.; Chabalowski, C. F.; Frisch, M. J. *J. Phys. Chem.* **1994**, *98*, 11623.
(18) Chai, J.-D.; Head-Gordon, M. *Phys. Chem. Chem. Phys.* **2008**, *10*, 6615.
(19) Zhao, Y.; Truhlar, D. *Theor. Chem. Acc.* **2008**, *120*, 215.
(20) Weigend, F.; Ahlrichs, R. *Phys. Chem. Chem. Phys.* **2005**, *7*, 3297.
(21) Tomasi, J.; Mennucci, B.; Cammi, R. *Chem. Rev.* **2005**, *105*, 2999.
(22) Simoń, L.; Goodman, J. M. *Org. Biomol. Chem.* **2011**, *9*, 689.
(23) Wiberg, K. B. *J. Org. Chem.* **2003**, *68*, 9322.
(24) Wang, H.; Houk, K. N. *Chem. Sci.* **2014**, *5*, 462.

DOI: 10.1021/jacs.5b12097
J. Am. Chem. Soc. 2016, 138, 503−506